

## Characterization Techniques

### *SAXS and WAXS*

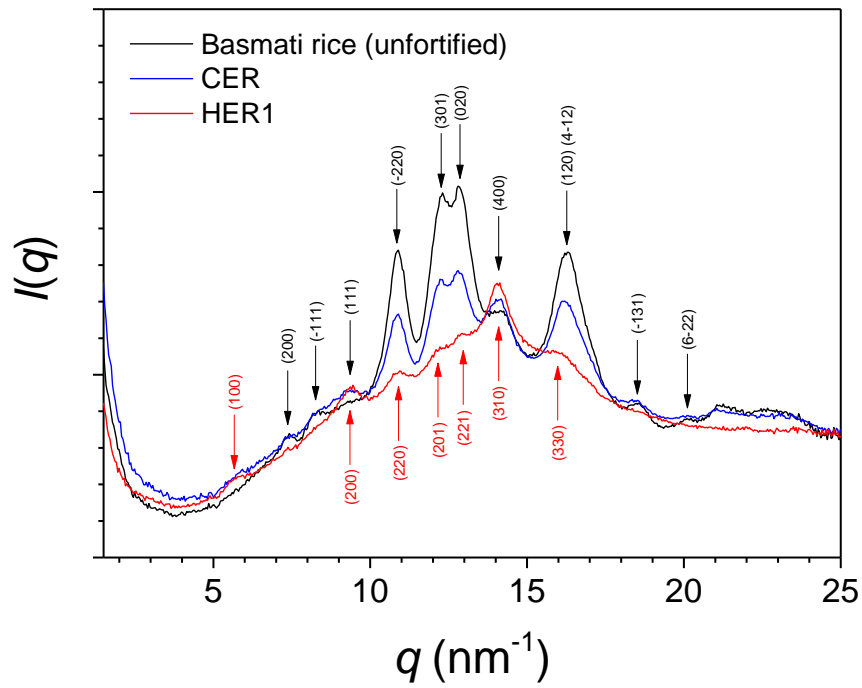
Small and wide-angle X-ray scattering (SAXS and WAXS) experiments were performed using a Bruker AXS Micro equipped with a microfocused beam (50 W, 50 kV, 1 mA) with the  $\lambda_{\text{CuK}\alpha} = 0.15418$  nm radiation in order to obtain direct information on the scattering patterns. The scattering intensities were collected by a Dectris 2D Pilatus 100K X-ray detector (83.8 cm  $\times$  33.5 cm, 172  $\mu\text{m}$  resolution resolution). An effective scattering vector range of  $0.1 \text{ nm}^{-1} < q < 25 \text{ nm}^{-1}$  was obtained, where  $q$  is the scattering wave vector defined as  $q = 4\pi \sin \theta / \lambda_{\text{CuK}\alpha}$  with a scattering angle of  $2\theta$ . Entire rice kernels were measured at room temperature. Deconvolution of the WAXS scattering profile allows for the evaluation of the degree of crystallinity which is defined as the ratio between the total area corresponding to the crystalline diffraction peaks and the total area under the scattering curve,  $\chi = A_{\text{crystalline}}/A_{\text{total}}$  [32]. Moreover, the presence of diffraction peaks at specific  $q$ -values allows for the unambiguous assignment of the starch polymorphism and the determination of the unit cell (1). The evaluation of the SAXS scattering peak and the adjustment of this peak by the paracrystalline model (2) allows for the evaluation of the semi-crystalline lamellar distance and size domain, as well as for the determination of the crystalline and amorphous layer thickness within the domain.

### *Differential scanning calorimetry*

Differential scanning calorimetry experiments were conducted on a Mettler Toledo DSC1 STAR<sup>e</sup> System apparatus in a temperature range from 25 to 90 °C at heating and cooling rates of 5 K min<sup>-1</sup> under nitrogen atmosphere. Milled rice kernel flour was mixed with water (1:10) and 40  $\mu\text{L}$  aluminum pans were used.

*Texture analysis*

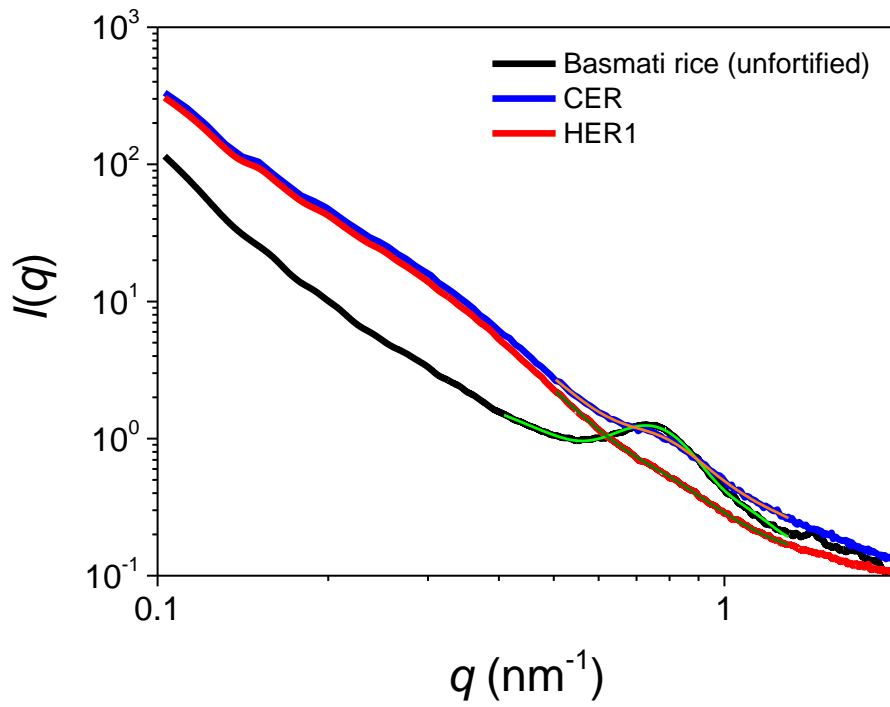
The mechanical properties of cooked rice were measured in compression mode using a universal tensile testing Zwick Z010 machine equipped with a 10 N load cell at the strain rate of 50 mm min<sup>-1</sup>. The measurements were performed per triplicate at room temperature after cooling the mixtures of rice kernels in water (1:4) which were cooked at 120 °C for 17.5 min at 8 °C for 15 min.



**Supplemental Figure 1.** 1D WAXS intensity profile for unfortified basmati rice (black), iron fortified cold extruded rice (CER, blue), and iron fortified hot extruded rice (HER1, red), with the indexation of the diffraction peaks (in black and blue: A-type; in red: V-type),  $n = 1$ .

**Supplemental Table 1.** Average degrees of crystallinity ( $\chi$ ), polymorphism, and lattice parameters ( $a$ ,  $b$ ,  $c$ , and  $\gamma$ ) evaluated from the WAXS intensity profiles,  $n = 1$ .

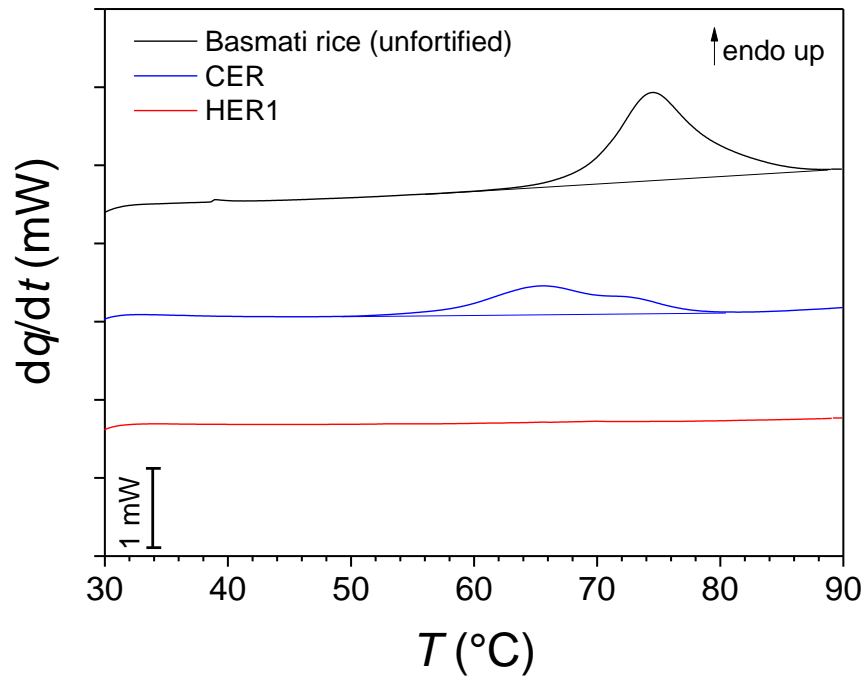
Sample	$\chi$ (%)	<i>polymorphism</i>	$a$ (Å)	$b$ (Å)	$c$ (Å)	$\gamma$ (deg)
Basmati rice	54	A (monoclinic)	20.5	11.4	11.9	120
Cold Extruded	49	A (monoclinic)	20.4	11.4	12.0	120
Hot Extruded	21	V (orthorhombic)	12.8	28.9	8.9	90



**Supplemental Figure 2.** 1D SAXS intensity profile for the unfortified basmati rice (black), the iron fortified cold extruded rice (CER, blue), and the iron fortified hot extruded rice (HER1, red), with the corresponding fitting curves,  $n = 1$ .

**Supplemental Table 2.** SAXS peak ( $q$ ), lamellar distance ( $d$ ), correlation length ( $\xi$ ), crystalline layer thickness ( $L_{\text{crystalline}}$ ), amorphous layer thickness ( $L_{\text{amorphous}}$ ), degree of crystallinity ( $\chi$ ) in the semi-crystalline domain evaluated from the SAXS intensity profiles,  $n = 1$ .

Sample	$q$ (nm <sup>-1</sup> )	$d$ (nm)	$\xi$ (nm)	$L_{\text{crystalline}}$ (nm)	$L_{\text{amorphous}}$ (nm)	$\chi$ (%)
Basmati rice	0.75	8.4	21	5.8	2.7	68
Cold Extruded	0.79	7.9	19	4.0	3.9	50
Hot Extruded	0.84	7.5	21	5.6	1.9	75

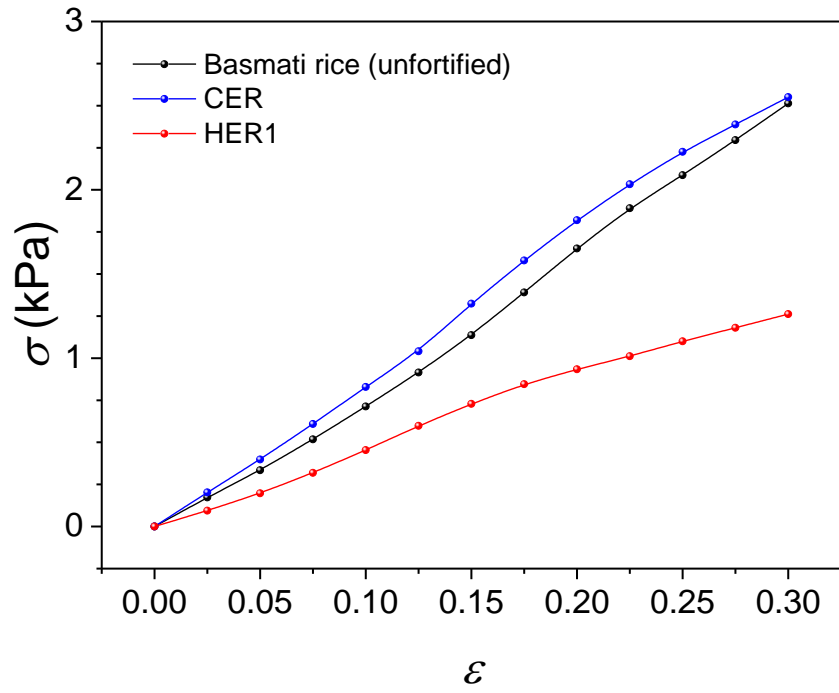


**Supplemental Figure 3.** Differential scanning calorimetry thermograms from 25 to 90  $^{\circ}\text{C}$  at 5  $\text{K min}^{-1}$  for the unfortified basmati rice (black), the iron fortified cold extruded rice (CER, blue), and the iron fortified hot extruded rice (HER1, red) mixtures with water (1:10),  $n = 1$ .

**Supplemental Table 3.** Onset ( $T_{\text{onset}}$ ) and maximum heat flow temperature ( $T_{\text{max}}$ ) evaluated from the Differential scanning calorimetry curves,  $n = 1$ .

Sample	$T_{\text{onset}}$ (°C)	$T_{\text{max}}$ (°C)
Basmati rice	69	74
Cold Extruded	57	66
Hot Extruded	-	not detectable





**Supplemental Figure 4.** Stress-strain curves in compression mode for the unfortified basmati rice (black), the iron fortified cold extruded rice (CER, blue), and the iron fortified hot extruded rice (HER1, red) after cooking the rice kernels in water (1:4),  $n = 1$ .

**Supplemental Table 4.** Elastic modulus ( $E$ ) evaluated from the stress-strain curves,  $n = 1$ .

Sample	$E$ (kPa)
Basmati rice	$6 \pm 1$
Cold Extruded	$7 \pm 1$
Hot Extruded	$4 \pm 1$

### Supplemental References

1. Kong L, Lee C, Kim SH, Ziegler GR. Characterization of starch polymorphic structures using vibrational sum frequency generation spectroscopy. *The Journal of Physical Chemistry B*. 2014;118:1775-83.
2. Yuryev VP, Krivandin AV, Kiseleva VI, Wasserman LA, Genkina NK, Fornal J, Blaszcak W, Schiraldi A. Structural parameters of amylopectin clusters and semi-crystalline growth rings in wheat starches with different amylose content. *Carbohydrate Research*. 2004;339:2683-91.